Selective Electroless Plating of Copper on (100)-Oriented Single Crystal Silicon Surface Modified by UV-Induced Coupling of 4-Vinylpyridine with the H-Terminated Silicon

D. Xu, E. T. Kang,* and K. G. Neoh

Department of Chemical Engineering, National University of Singapore, Kent Ridge, Singapore 119260

Yan Zhang, A. A. O. Tay, and S. S. Ang

Department of Mechanical Engineering, National University of Singapore, Kent Ridge, Singapore 119260

M. C. Y. Lo and K. Vaidyanathan

Institute of Microelectronics, 11 Science Park Road, Singapore Science Park Π, Singapore 117685

A Sn-free electroless plating process for producing patterned and adherent copper deposits on (100)-oriented single-crystal silicon substrates is described. Pristine and resist-patterned Si(100) substrates were etched, initially, by aqueous HF to produce the hydrogen-terminated silicon surfaces (H–Si(100) surfaces). The H–Si(100) surfaces were further functionalized by the UV-induced reactive coupling of 4-vinylpyridine (4VP). The composition and topography of the modified Si(100) surfaces were characterized by X-ray photoelectron spectroscopy and atomic force microscopy, respectively. The coupled 4VP layer exhibited good stability in boiling chloroform, boiling water, sonicating dichloromethane, aqueous solution of HF and aqueous solution of KOH. Not only did the 4VP layer provide chemisorption sites for the palladium complexes without the need for prior sensitization in $SnCl_2$ solution during the electroless plating process but it also served as the adhesion promotion layer and diffusion barrier for the electrolessly deposited copper. The 180°-peel adhesion strength of the electroless deposited copper on the modified silicon surface was dependent on the extent of 4VP surface coverage and could reach about 4 N/cm.

1. Introduction

Copper is rapidly replacing aluminum in metal interconnects in the ultra-large scale integration (ULSI) technology because of its lower resistivity and its potentially higher resistance to electron migration and stress-induced voiding.[1–4] Copper can be deposited by plasma vapor deposition (PVD), laser-induced reflow, chemical vapor deposition (CVD), electroless deposition, and electroplating.[5,6] The electroless deposition technique is especially appealing because of its low cost, inherent selectivity and ability to deposit high quality films on very thin seed layers.[7–11] Palladium is one of the most commonly used catalysts for the electroless plating process. However, palladium cannot be chemisorbed on the silicon and other inert substrate surfaces without the prior sensitization of these surfaces by a tin compund, such as $SnCl_2$.[11] In addition, the adhesion of the electrolessly deposited copper to the pristine silicon surface is inherently poor. Thus, subjecting the silicon substrate surface to an effective pretreatment prior to the electroless metallization process is a necessary and essential step. The methods for the modification of silicon surfaces have included chemical etching,[7–10] plasma immersion ion implantation,[12–14] chemical vapor deposition,[15,16] dry seeding via sputtering,[17] coupling of silane-based and self-assembled monolayers (SAMs),[18,19] plasma graft polymerization,[20] etc. Earlier studies have also demonstrated that palladium chemisorption can be achieved directly on polymer surfaces modified by plasma-induced grafting of

nitrogenated groups.[21,22] It has also been shown that self-assembled films of organosilanes containing ligand functional groups, such as phosphines, pyridines, or alkylamines, are useful for binding palladium catalysts to silicon surfaces and that the bound catalysts initiate electroless metal deposition.[18, 23]

Chemical modification of silicon surfaces via the deposition and patterning of organic and inorganic layers is currently of great research interest.[24,25] One of the most important advances involves the formation of monolayers by the reaction of alkenes with the hydrogen-terminated silicon surface, using either free radical initiation or ultraviolet activation.[26–28] Boukherroub et al.,[29] on the other hand, have used the Lewis acid-catalyzed hydrosilylation of alkenes and the direct reaction of alkylmagnesium. The preparation of highly stable monolayers on the hydrogen-terminated Si(100) surfaces, using both the functionalized and nonfunctionalized alkenes, has also been reported.[30] Lee et al. modified the hydrogen-terminated surface of porous and single-crystal n-type silicon by photoelectrochemical reaction with carboxylic acids, resulting in the formation of surface-bonded silyl esters.[31] However, the covalent attachment of N-containing organic layers to the hydrogen-terminated silicon surfaces is yet to be explored in detail. A N-containing layer on the silicon surface can provide potential chemisorption sites for the palladium catalyst in the electroless plating process. On the other hand, selective metallization can be achieved either by the selective deactivation of a catalytic substrate or by the selective activation of a nonreactive surface by a catalyst.[32] Several methods for producing patterned catalysts are known. Most of these methods are based on photolithographic tech-

* To whom all correspondence should be addressed. Phone: +65-6874-2189. Fax:+65-6779-1936. E-mail: cheket@nus.edu.sg.

Selective Electroless Plating of Copper

J. Phys. Chem. B, Vol. 106, No. 48, 2002 **12509**

niques.[33,34] An alternative route to selective metallization is chemical vapor deposition.[35,36]

In this work, N-containing molecular layers, tethered via covalent Si−C bonds, are incorporated onto the hydrogen-terminated Si(100) wafer surfaces via the UV-induced coupling of 4-vinylpyridine (4VP). The 4VP layers are activated directly in PdCl₂ solution, in the absence of prior sensitization by SnCl₂, for the subsequent electroless plating of copper. Selective metallization is achieved using the resist-patterned silicon substrates. The combination of these techniques yields a simple, effective, and Sn-free method for producing adherent copper layers on silicon substrates, either uniformly or in selective micro-patterns.

2. Experimental Section

2.1. Materials. (100)-oriented single-crystal silicon or Si-(100) wafers, having a thickness of about 2 mm and a diameter of 150 mm, were obtained from Unisil Co. of Santa Clara, CA. The as-received wafers were polished on one side and doped as n-type. The silicon wafers were sliced into rectangular strips of about 3 cm × 1 cm in size. To remove the organic residues on the surface, the silicon substrate was washed with the "piranha" solution, a mixture of 98 wt % concentrated sulfuric acid (70 vol %) and hydrogen peroxide (30 vol %).[37] The silicon substrates were immersed in the piranha solution for about 30 min at 60 °C. After rinsing with copious amounts of doubly distilled water, the silicon strips were dried at 80 °C in a vacuum oven for 1 h. 4-vinylpyridine (4VP) was purchased from the Aldrich Chemical Co. of Milwaukee, WI and was purified by vacuum distillation before use. Micropatterned silicon wafers were prepared by the conventional photolithographic process, using a negative resist and a photomask. The patterned wafers were also sliced into rectangular strips of about 3 cm × 1 cm in size.

2.2. HF Acid Etching and UV-Induced Coupling of the 4VP Layer. A 10 vol % hydrofluoric acid solution was deoxygenated by sparging with argon for 30 min through a Teflon tube inserted into the solution. The pristine silicon strips or the patterned siliocon strips were immersed in the hydrofluoric acid solution in individual Teflon vials. A 5 min immersion time was sufficient to remove the oxide film and to leave behind a uniform H-terminated Si(100) surface.[38] The silicon strip with a H-terminated surface was placed immediately in a Pyrex tube containing 5 mL of 20 vol % ethanol or hexane solution of 4VP. After purging with purified argon for about 30 min, the reaction mixture was sealed with a silicon rubber stopper. It was then subjected to UV irradiation in a Riko RH400-10 W rotary photochemical reactor (manufactured by Riko Denki Kogyo of Chiba, Japan). The reactor was equipped with a 1000 W high-pressure Hg lamp and a constant-temperature bath. All UV-induced reactions were carried out at a constant temperature of 28 °C. After the UV irradiation for a predetermined period of time, the surface modified silicon substrate was removed from the 4VP solution and washed thoroughly with copious amounts of ethanol to remove the residual 4VP and adsorbed oligomers.

2.3. Electroless Plating of Copper on the 4VP−Modified Silicon Surfaces and the Adhesion Strength Measurements. The 4VP-modified silicon surfaces were activated, either in the presence or absence of prior sensitization by SnCl₂, through the immobilization of palladium catalyst for the subsequent electroless plating of copper. For surface activation in the absence of prior sensitization by SnCl₂, the 4VP-modified silicon substrate was immersed directly in an aqueous solution containing 0.1 wt % PdCl₂ and 1.0 wt % HCl (12 M) for 10 min, followed by rinsing with copious amounts of doubly distilled water. The surface activated silicon substrate was then immersed in an electroless copper plating bath for about 4 min to achieve a thickness of about 0.6 μm. The composition of the copper plating bath was as follow: 7 g/L of CuSO₄·5H₂O, 25 g/L of potassium sodium tartrate, 4.5 g/L of sodium hydroxide, and 9.5 g/L of formaldehyde.[39] The Cu-metallized silicon strip was then rinsed thoroughly with copious amounts of doubly distilled water.

The metallized silicon strip was adhered to a copper sheet backing (0.1 mm in thickness), using an epoxide adhesive (Araldite Stand, from Ciba Specialty Chemical Co. of Duxford, Cambridge, England), for the subsequent 180°-peel adhesion strength measurement. The assembly was thermally cured in a vacuum oven at 120 °C for 3 h prior to the 180°-peel adhesion test. The 180°-peel adhesion strength measurements were carried out at room temperature on an Instron 5544 tensile tester. All measurements were carried out at a crosshead speed of 10 mm/min. For each peel adhesion strength reported, at least three sample measurements with variation within ±0.5 N/cm were averaged.

For comparison purpose, activation of the pristine Si(100) and 4VP-modified silicon surfaces was also carried out via the conventional two-step process.[39] For this process, the pristine Si(100) and the 4VP-modified silicon surfaces were first sensitized in an aqueous solution containing 0.3 wt % SnCl₂ and 2.5 wt % HCl (12M) for 2 min, followed by rinsing with doubly distilled water. The subsequent activation in PdCl₂ solution, electroless plating of copper, attachment of the copper sheet backing, thermal posttreatment, and adhesion strength measurement were similar to those described above.

2.4. Surface Characterization. The chemical composition of the pristine, H-terminated, and 4VP-modified Si(100) surfaces was determined by X-ray photoelectron spectroscopy (XPS). The XPS measurements were performed on a Kratos AXIS HSI spectrometer using a monochromotized Al Kα X-ray source (1486.6 eV photons) at a constant dwell time of 100 ms and a pass energy of 40 eV. The samples were mounted on the standard sample studs by means of double-sided adhesive tapes. The core-level signals were obtained at a photoelectron takeoff angle (α, measured with respect to the sample surface) of 90°. The X-ray source was run at a reduced power of 150 W (15 kV and 10 mA). The pressure in the analysis chamber was maintained at 10^{-8} Torr or lower during each measurement. All binding energies (BEs) were referenced to the C 1s hydrocarbon peak at 284.6 eV. Surface elemental stoichiometries were determined from XPS spectral area ratios, after correcting with the experimentally determined sensitivity factors, and were reliable to within ±5%. The elemental sensitivity factors were calibrated using stable binary compounds of well-established stoichiometries.

The topographies of the H-terminated and 4VP-modified silicon surfaces were studied by atomic force microscopy (AFM), using a Nanoscope IIIa AFM from the Digital Instrument Inc. In each case, an area of 5 × 5 um square was scanned using the tapping mode. The drive frequency was 330 ± 50 kHz, and the voltage was between 3 and 4.0 V. The drive amplitude was about 300 mV, and the scan rate was 0.5−1.0 Hz. An arithmetic mean of the surface roughness (R_a) was calculated from the roughness profile determined by AFM.

Static water contact angles of the H-terminated and 4VP-modified silicon surface were measured at 25 °C and 60% relative humidity by the sessile drop method, using a 3 μL water
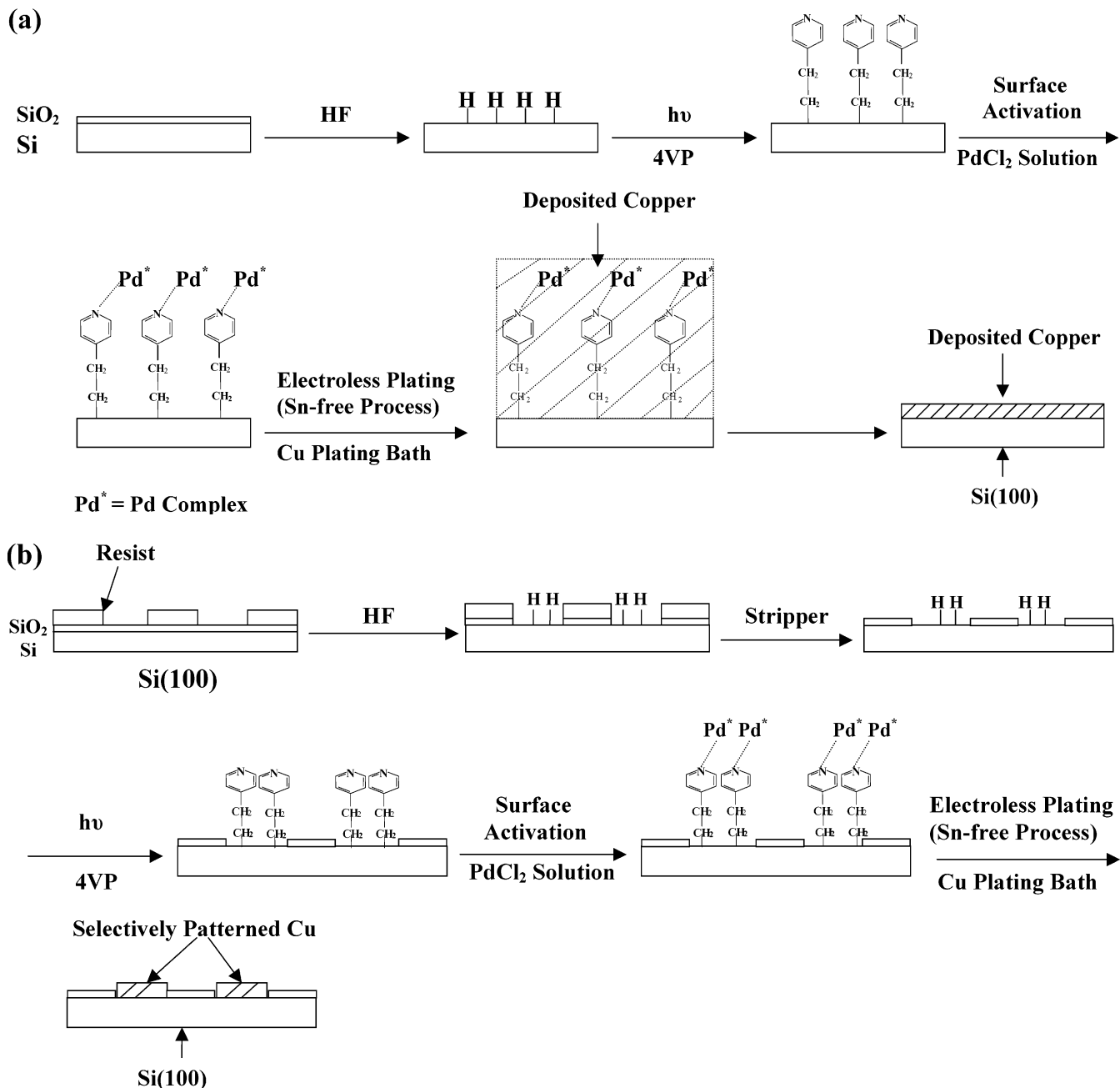
Figure 1. Schematic diagram illustrating the process of HF acid etching, UV-induced coupling, surface activation, and electroless plating of copper on (a) the blank Si(100) surface and (b) the resist-patterned Si(100) surface.

droplet in a telescopic goniometer (Rame-Hart, model 100-00-(230), manufactured by the Rame-Hart, Inc. of Mountain Lakes, NJ). The telescope with a magnification power of 23× was equipped with a protractor of 1° graduation. For each sample, at least five measurements from different surface locations were averaged. Each angle reported was reliable to ±3°.

Scanning electron microscopic (SEM) images and energy-dispersive X-ray (EDX) analyses were obtained from the JEOL 6320 electron microscope. The samples were mounted on the sample studs by means of double-sided adhesive tapes. The SEM measurements and EDX analyses were performed at an accelerating voltage of 15 kV.

3. Results and Discussion

The processes of HF acid etching of the Si(100) substrate to produce the H-terminated surface (H−Si(100) surface), UV-induced coupling of 4VP on the H−Si(100) surface, the surface

activation by $PdCl_2$ in the absence of prior sensitization by $SnCl_2$, and the electroless plating of copper are shown schematically in Figure 1a. The details of each process are discussed below.

3.1. UV-Induced Coupling of 4VP on the H−Si(100) Surface. Figure 2 shows the respective XPS wide scan spectra of the freshly prepared H−Si(100) surface (part a) and the H−Si(100) surfaces after UV-irradiation for 20 min in Ar-purged hexane (part b), in 20 vol % Ar-purged hexane solution of 4VP (part c), in Ar-purged ethanol (part d), in 20 vol % Ar-purged ethanol solution of 4VP (part e) and in Ar-purged neat 4VP (part f). The line shape of the Si 2p core-level spectrum of the H−Si(100) surface confirms that the silicon surface is ideally H-terminated after the HF treatment, because no oxidized silicon in the binding energy (BE) region of 101−103.5 eV can be detected (see Figure 3b below). The O 1s signal observed for the H−Si(100) sample in Figure 2a is probably associated

Selective Electroless Plating of Copper

J. Phys. Chem. B, Vol. 106, No. 48, 2002 **12511**
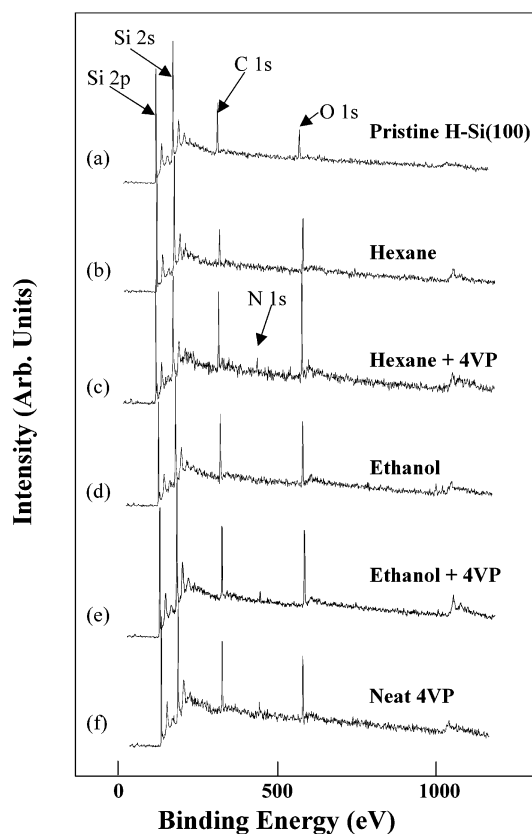
Figure 2. XPS wide scan spectra of (a) the freshly prepared H−Si-(100) surface and (b) the H−Si(100) surfaces after UV-irradiation for 20 min in hexane, (c) in 20 vol % hexane solution of 4VP, (d) in ethanol, (e) in 20 vol % ethanol solution of 4VP, and (f) in neat 4VP. (All systems were purged by argon.)

with the adventitious carbon materials, the presence of which is indicated by the weak C 1s signal. The H-terminated silicon surface, being a reactive surface, can react with other oxygen-containing nucleophiles, such as water, alcohols, and acids under mild conditions.[31,40−44] The presence of the UV-coupled 4VP layer on the Si(100) surface can be deduced from the appearance of a strong N 1s core-level signal at the BE of about 398.5 eV (Figure 2 parts c, e, and f), attributable to the imine (−N=) species of 4VP.[45] The strong Si signals in the wide scan spectra of Figure 2 parts c, e, and f suggest that the thickness of the coupled 4VP layer is much less than the sampling depth of the XPS technique (about 7.5 nm in an organic matrix[20]).

In the present study, the effect of solvent on the properties of the coupled 4VP layers were also investigated by XPS. Hexane and ethanol were chosen as solvents for 4VP. Initially, the H−Si(100) substrate was irradiated by the UV source for 20 min while immersed in the Ar-purged hexane (Figure 2b) or ethanol (Figure 2d). It can be observed that UV irradiation of the H−Si(100) surface in ethanol results in a much higher [C]/[Si] ratio than in hexane. The result suggests the presence of reactions between ethanol and the H-terminated surface. In the cases of the H−Si(100) surfaces irradiated in the hexane or ethanol solution of 4VP or in neat 4VP, the wide scan spectra of the resulting silicon surfaces have similar features, except that the [O]/[Si] ratio is somewhat higher when hexane is used as the solvent for 4VP (see below).

3.2. Effect of Reaction Conditions on the 4VP Coverage of the Silicon Surface. Figure 3 shows the N 1s and Si 2p core-level spectra of the pristine H−Si(100) surface (parts a and b), the surfaces prepared by the photochemical reaction of H−Si(100) in 20 vol % hexane solution of 4VP (parts c and
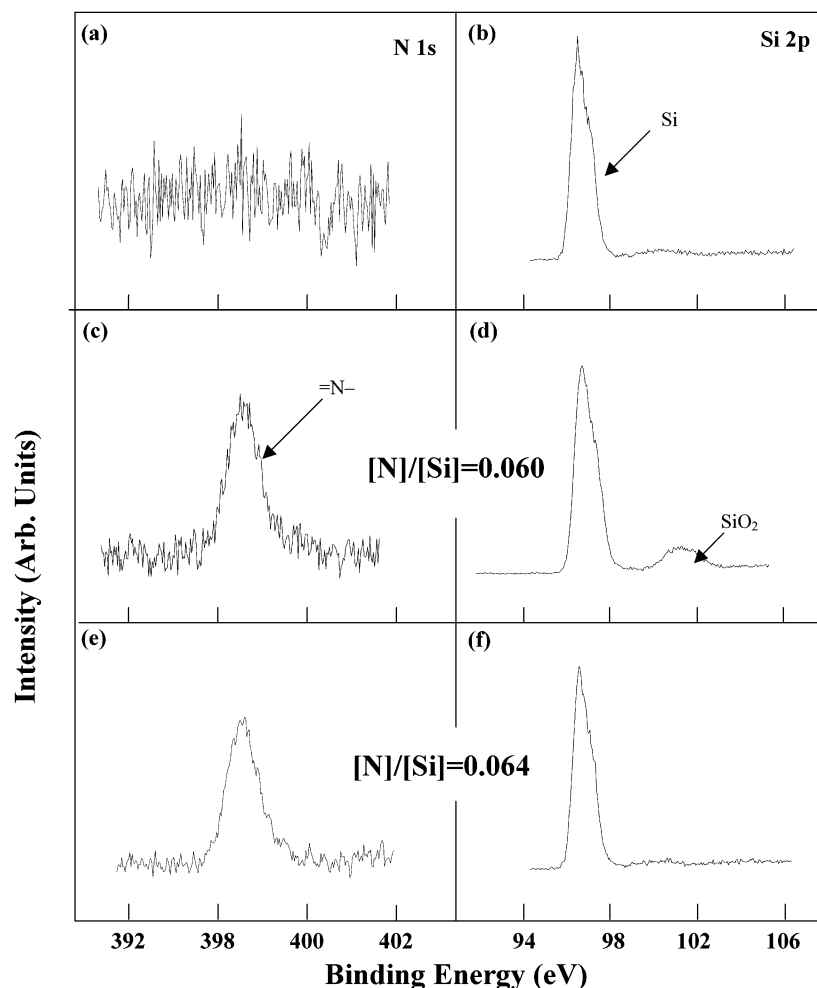
d), and in 20 vol % ethanol solution of 4VP (part e and f). The 4VP coverage in each case can be expressed simply as the surface [N]/[Si] ratio, because each 4VP unit contains one nitrogen atom. The silicon surface shows a certain level of oxidation when hexane is used as the solvent, as suggested by the appearance of a weak Si 2p core-level peak component at the BE of about 102 eV, attributable to the SiO$_2$ species (Figure 3d). The slightly lower [N]/[Si] ratio or less uniform coverage of 4VP on the sample surface prepared in hexane solution probably has resulted in a small extent of oxidation of the silicon surface during the subsequent washing and drying process. In addition, the finite extent of reaction between ethanol and the H−Si(100) surface (see Figure 2d) probably has contributed to the passivation of the remaining active sites after the photochemical reaction with 4VP.

Figure 4 shows the 4VP coverage on the silicon surface, expressed as the [N]/[Si] ratio, as a function of the UV irradiation time. The photochemical reactions were carried out in 20 vol % hexane or ethanol solutions of 4VP. The coverages reported at zero irradiation time are for the H−Si(100) substrates immersed in the Ar-purged ethanol and hexane solutions of 4VP for 1 h in the dark to allow for any equilibrium surface reaction to occur. In the absence of UV induction, almost no N 1s signal is discernible. Furthermore, a slightly higher 4VP coverage ([N]/[Si] ratio) is always obtained for the surface coupling reaction carried out in ethanol solution than in hexane solution under similar reaction conditions. The data in Figure 4 also show that the majority of the surface sites have reacted within the first 10 min of irradiation, regardless of the choice of solvent for 4VP. This observation suggests that prolonged UV irradiation does not introduce more 4VP molecules onto the silicon surface. In this work, the duration of UV exposure for the coupling of the 4VP layer was kept at 20 min to ensure complete reaction.

Figure 5 shows the dependence of the surface [N]/[Si] ratio on the 4VP concentration in ethanol and hexane used for the UV-induced coupling reaction. It is clear that the concentration of 4VP solution has almost no effect on the [N]/[Si] ratio for 4VP solution concentrations above 20 vol %. Even when ethanol is used as a solvent, its finite reactivity toward the H-terminated silicon surface does not seem to interfere with the reaction between 4VP and the H−Si(100) surface. In addition, pure 4VP does not give rise to a higher surface coverage than the 4VP solutions. Thus, for 4VP concentrations above 20 vol %, the reaction of 4VP with the H-terminated silicon surface is not diffusion limited.

Cicero et al.[46] proposed a simplified mechanism for the formation of alkyl monolayers on H-terminated silicon surfaces. The radical sites (i.e., dangling bonds), formed by reaction with radicals or by direct irradiation, react with alkenes to form a surface-bonded alkyl radical. This radical in turn abstracts a hydrogen atom from an adjacent Si−H bond, thus saturating the alkyl group and creating another reactive silicon radical. The reaction then proceeds as a chain reaction propagating along the surface. As is known for the free radical addition of molecular silyl radicals to terminal olefins, the exclusive addition of the silicon radical to the α-carbon of the terminal olefin occurs readily due to steric reasons. The incipient secondary radical on the β-carbon allows for a sterically favored six-member transition state during the abstraction of a neighboring surface hydrogen atom. Such a quenching of the secondary carbon radical may explain the lack of a significant degree of polymerization. The coverage never exceeds one monolayer even with styrene, a molecule that polymerizes readily.[46] Thus, the
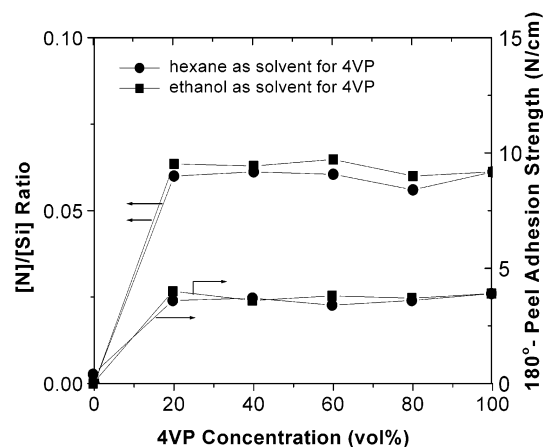
Figure 3. N(1s) and Si(2p) core-level spectra of the as-prepared H−Si(100) surface (a and b) and of the surfaces prepared by the photochemical reaction of H−Si(100) in (c and d) 20 vol % hexane solution of 4VP and (e and f) 20 vol % ethanol solution of 4VP.
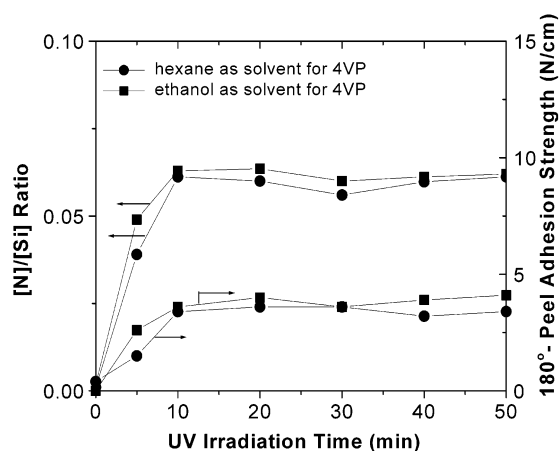
Figure 4. Effect of UV irradiation time on the graft concentration and the 180°-peel adhesion strength of the electrolessly deposited copper with the 4VP-modified silicon surface (4VP concentration = 20 vol %, from the Sn-free process).


Figure 5. Effect of 4VP concentration on the graft concentration and the 180°-peel adhesion strength of the electrolessly deposited copper with the 4VP-modified silicon surface (UV irradiation time =20 min, from the Sn-free process.)

mechanism of the UV-induced reaction of 4VP with H−Si-(100) probably proceeds by the same path as that of the olefins, especially that of styrene (Figure 6). However, a more complicated situation may arise with 4VP. In addition to the steric effect, the pyridine group, which is supposed to stand along outside the 4VP layer, may not allow for the dense packing of the 4VP molecules on the silicon surface because of its own cationic nature and the repulsion of other pyridine units. This

effect accounts for the low [N]/[Si] ratio (about 0.06 in Figure 4) even in the case of reaction with pure 4VP. It can be deduced that the remaining interstitial spaces on the H-terminated silicon surface provide reaction sites for the less reactive solvent molecules. As a result, the solvent shows almost no effect on the surface coverage.

3.3. Chemical Stability of the 4VP−Modified Silicon Surfaces. The measurement of water contact angles is a quick

Selective Electroless Plating of Copper

J. Phys. Chem. B, Vol. 106, No. 48, 2002 **12513**
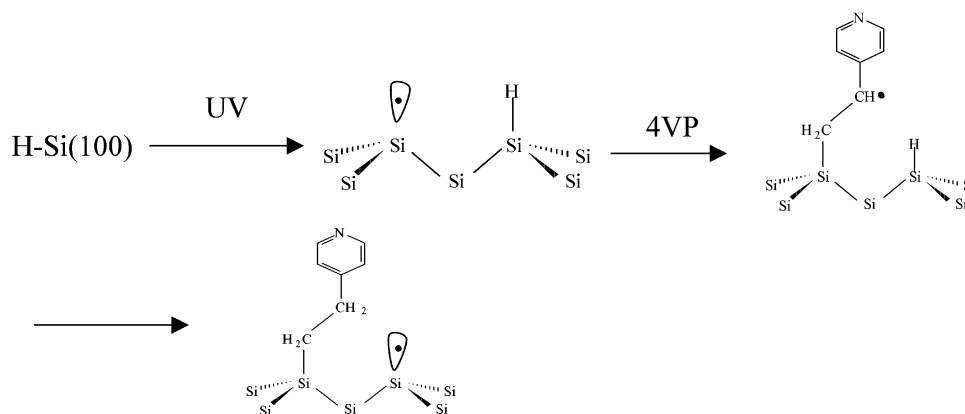
Figure 6. Photoinitiated free radical mechanism for the reaction of H−Si(100) surface with 4-vinylpyridine. The dangling bonds on the silicon surface are formed by UV irradiation. 4VP reacts with the dangling bond to form a secondary carbon radical that abstracts the neighboring hydrogen to produce a new surface dangling bond.

TABLE 1: Water Contact Angle Measurements

surfaces	water contact angle ($\pm3°$)
pristine Si(100)	25°
H-terminated Si(100)	72°
as-prepared 4VP-modified Si[a]	60°
4VP-modified Si after exposure to air for a week	60°
4VP-modified Si after exposure to air for a month	60°

[a] From UV-induced coupling of 4VP on H-terminated Si(100) surface. ([N]/[Si] = 0.064).

TABLE 2: [N]/[Si] Ratio of the 4VP-Modified H−Si(100) Surface[a] After the Various Stability Tests

surface treatment	[N]/[Si] ratio (%)[b]
1. sonication in dichloromethane for 5 min	constant
2. immersion in boiling choloroform for 1 h	constant
3. immersion in boiling water for 1 h	constant
4. treatment 1 + 2 + 3	constant
5. immersion in distilled water for 3 days,	constant
6. immersion in deoxygenated 10% aqueous HF for 1 h	90%
7. immersion in 1 M KOH for 10 min	constant
8. immersion in 1 M KOH for 16 h	0%

[a] UV irradiation time = 20 min, in 20 vol % ethanol solution of 4VP. [N]/[Si] = 0.064. [b] Compared to the sample's original [N]/[Si] value.
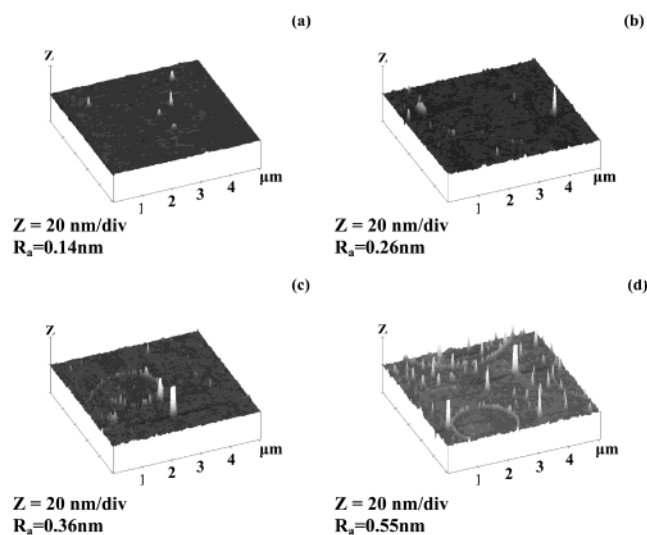
and useful tool in monolayer analysis. The water contact angle measurements have a surface sensitivity of 1 nm or less,[47] in comparison to a probing depth of about 7.5 nm for the XPS technique in an organic matrix.[48] It can also be used to investigate the 4VP layer stability in the present study, when measured as a function of time. As shown in Table 1, the water contact angle of 4VP-modified silicon surface is about 60°, indicating a somewhat hydrophobic nature of the 4VP layer. The water contact angle of the 4VP-modified H−Si(100) surface does not change appreciably even after several weeks of exposure to air.

In the absence of direct spectroscopic evidence, chemical robustness is often taken as an indirect evidence for the presence of covalent linkages. To test the stability of the surface layers, the 4VP-modified silicon surfaces, which had already been washed exhaustively in ethanol after preparation, were subjected to the following treatments: (1) sonication in dichloromethane for 5 min; (2) immersion in boiling chloroform for 1 h; (3) immersion in boiling water for 1 h; (4) combination of treatments 1, 2, and 3; (5) immersion in distilled water for 3 days; (6) immersion in deoxygenated 10% aqueous HF for 1 h; (7) immersion in 1 M KOH for 10 min; and (8) immersion in 1 M KOH for 16 h.[26] The results of the treatments are summarized in Table 2. It is obvious that the ultrathin 4VP layers are very robust. The first four treatments did not have any measurable effect on the stability of the 4VP layer on the silicon surface. Successive washing with dichloromethane and chloroform, even at room temperature would have removed completely the physically adsorbed 4VP from the surface. Treatment with degassed 10% aqueous HF solution for 1 h led to a decrease in [N]/[Si] ratio of about 10%. Immersion in 1 M KOH for 10 min did not have any effect on [N]/[Si] ratio of the surface. Nevertheless, the KOH treatment is particularly aggressive. After exposure to 1 M KOH for 16 h, the N 1s signal was no longer discernible, suggesting the complete removal of the 4VP layer. The good stability of the 4VP-modified H−Si(100) surface is

Figure 7. Topography of (a) the freshly prepared H−Si(100) surface and the 4VP-modified silicon surface prepared by the photochemical reaction of H−Si(100) with (b) neat 4VP, (c) 20 vol % ethanol solution of 4VP, and (d) 20 vol % hexane solution of 4VP.

comparable to that of the H−Si(111) surface modified by an alkyl monolayer.[25,29] Thus, chemical coupling, and not physisorption, of the 4VP layer on the silicon substrate must have occurred.

3.4. Topography of the 4VP-Modified H−Si(100) Surfaces. The changes in topography of the silicon surfaces after modification by UV-induced coupling with 4VP are studied by AFM. Figure 7 shows the respective AFM images of the freshly prepared H−Si(100) surface (part a) and of the 4VP-modified

TABLE 3: Effect of Surface Modification of the Si(100) Substrate on the Adhesion Strength of the Electrolessly Deposited Copper

surface modification	activation method	180°-peel adhesion strength (N/cm)
H-terminated Si surface (H−Si(100)	two-step process[c]	0.3 ± 0.2
4VP-modified H−Si(100)[a]	two-step process	3.3 ± 0.5
4VP-modified H−Si(100)[a]	Sn-free process[d]	3.6 ± 0.5
4VP-modified H−Si(100)[b]	two-step process	2.9 ± 0.5
4VP-modified H−Si(100)[b]	Sn-free process	4.0 ± 0.5

[a] UV-induced coupling of on the H−Si(100) surface. (UV irradiation time = 20 min, in 20 vol % hexane solution of 4VP.) [b] UV-induced preparation of 4VP on the H−Si(100) surface. (UV irradiation time = 20 min, in 20 vol % ethanol solution of 4VP.) [c] Sensitization in SnCl$_2$ solution, followed by activation in PdCl^2 solution. [d] Direct activation in PdCl$_2$ solution only.

silicon surfaces prepared by the photochemical reaction of H−Si(100) in neat 4VP (part b), in 20 vol % ethanol solution of 4VP (part c), and in 20 vol % hexane solution of 4VP (part d). The surface of the freshly prepared H−Si(100) is quite uniform and smooth, with a root-mean-square surface roughness value (R_a) of only about 0.14 nm. After the coupling of the 4VP layer in neat 4VP, the R_a value of the 4VP-modified surface increases slightly to about 0.26 nm, indicating the presence of a still very smooth surface after the coupling of the 4VP layer (Figure 7b). When the 20 vol % ethanol solution of 4VP is used for the coupling reaction, the surface topography changes more markedly, with the R_a value increases to about 0.36 nm (Figure 7c). This result suggests that, although the existence of solvent does not influence the deposition of the 4VP layer on the H−Si(100) surface, it does affect the surface topography, further confirming to the presence of reaction between the solvent and H−Si(100) surface. In the case of the 4VP-modified H−Si(100) surface prepared in hexane, the R_a value of surface increases further to about 0.55 nm (Figure 7d). As shown in Figure 3d earlier, this appreciably increase in surface roughness is, in part, due to the formation of SiO$_2$.

3.5. Adhesion Characteristics of the Electrolessly Plated Copper on the 4VP−Modified H−Si(100) Surface. Irrespective of the methods used (the Sn-free process or the two-step process) for surface activation and subsequent electroless deposition of copper, the ultimate adhesion strength between the metal and the silicon substrate is one of the primary concerns for the microelectronics applications. In this work, the adhesion strength of the electrolessly deposited copper with the silicon surfaces obtained via the Sn-free process and the two-step process are compared. As shown in Table 3, the 180°-peel adhesion strength of copper electrolessly deposited via the two-step process on the H−Si(100) surface is marginal or about 0.3 N/cm. The H−Si(100) surface cannot be activated in the absence of prior sensitization by SnCl$_2$. It is also obvious from Table 3 that the adhesion strength of the electrolessly deposited copper with the 4VP-modified H−Si(100) (either using hexane or ethanol as solvent for the coupling reaction), obtained via the Sn-free process, is higher than that obtained via the conventional two-step process. A 180°-peel adhesion strength of about 4 N/cm can be achieved for the electrolessly deposited copper with the present 4VP-modified H−Si(100) surface. The results are in general agreement with that reported earlier for the electrolessly deposited copper on poly(tetrafluoroethylene) and polyimide films modified by surface graft copolymerization with the N-containing monomers, including 4VP.[20,49] Previous studies have also indicated that not only do the nitrogen atoms in the
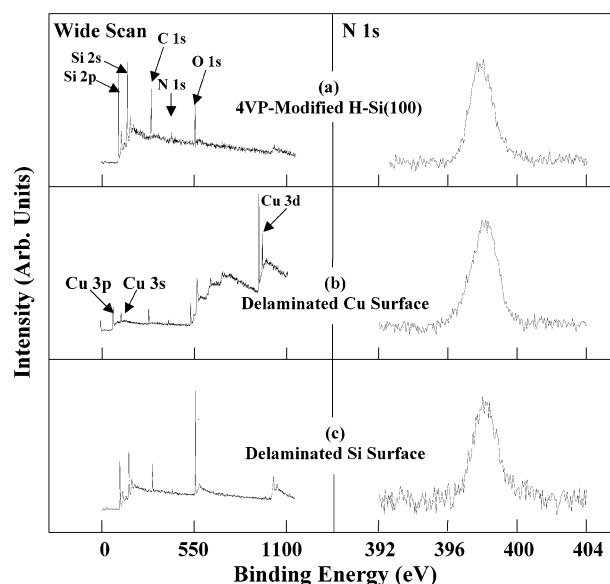
Figure 8. XPS wide scan and N 1s core-level spectra of (a) the 4VP-modified surface ([N]/[Si] ratio = 0.064) and of the delaminated (b) Cu and (c) Si surfaces from the corresponding Cu/4VP-modified Si assembly having a 180°-peel adhesion strength of about 4 N/cm.

pyridine rings of the 4VP polymer form charge transfer complexes with the Pd ions, they also interact directly with the electrolessly deposited copper to form the Cu−N bond,[50] which accounts for the strong adhesion of the metal to the substrate. On the other hand, in the two-step surface activation process, not only does the Sn species poison the palladium catalyst but it also reduces the bondability of the 4VP-modified silicon surface to the electrolessly deposited copper.[51] The increase in the 180°-peel adhesion strength of the electrolessly deposited copper with the 4VP-modified silicon surface coincides with the increase in the surface [N]/[Si] ratio, as shown in Figures 4 and 5. Thus, the contribution of the coupled 4VP layer to the adhesion of the electroless deposited copper with the silicon substrate is ascertained.

3.6. Adhesion Failure Mode. The adhesion failure mode of the Cu/Si interfaces, obtained from the electroless deposition of copper on the 4VP-modified H−Si(100) surfaces via the Sn-free process, is investigated by XPS. Figure 8 shows the respective wide scan and N 1s core-level of the 4VP-modified silicon surface, prior to the Pd activation and electroless deposition of copper (part a), and the delaminated copper surface (part b) and silicon surface (part c) from a Cu/4VP-midified H−Si(100) assembly having a 180°-peel adhesion strength of about 4 N/cm. The presence of the 4VP component on both of the delaminated surfaces is suggested by the fact that the N 1s core-level spectra of the delaminated copper and silicon surfaces are similar to that of the original 4VP modified silicon surface. No copper signal is discernible on the delaminated silicon surface. These observations suggest that the Cu/Si assembly must have delaminated by adhesional failure inside the 4VP layer. Furthermore, no copper diffusion across the 4VP layer has occurred, at least under the thermal curing conditions (180 °C for 3 h) of the present Cu/Si assembly (see the Experimental Section). This result suggests that the 4VP layer also serves, to some extent, as a diffusion barrier for the deposited copper. The strong adhesion of the electrolessly deposited copper to the 4VP-modified silicon substrate is attributable to the strong interaction of the pyridine functional groups of the coupled 4VP layer with palladium and copper atoms and the fact that the 4VP layer is covalently tethered on the silicon substrate surface.
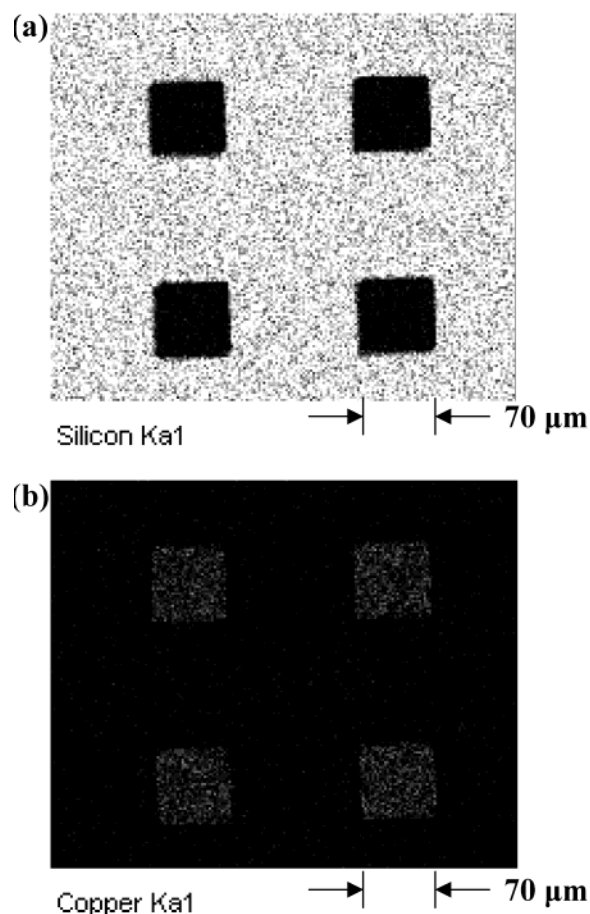
Selective Electroless Plating of Copper

J. Phys. Chem. B, Vol. 106, No. 48, 2002 **12515**
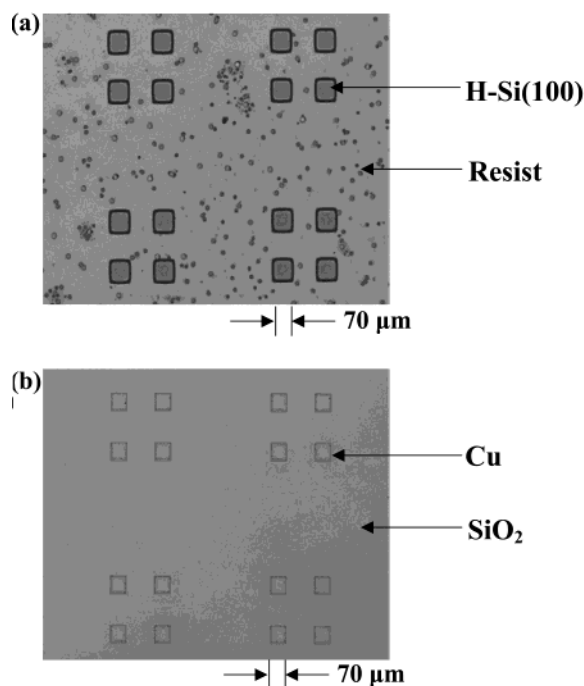
Figure 9. Optical micrograph of (a) the resist-patterned silicon surface and (b) selectively metallizaed silicon surface. The resist-patterned silicon was processed as described in Figure 1b.

3.7. Micropatterning of the Silicon Surfaces. The procedure for the selective electroless deposition of copper on the resist-patterned Si(100) surface is shown schematically in Figure 1b. Resist-patterned silicon substrate (Figure 9a) with square clearance (opening) of $70 \times 70 \ \mu m^2$ was first subjected to the HF etching, producing the H-terminated silicon surface only in the exposed regions. The resist on the silicon surface was subsequently removed by a stripper. The silicon substrate was transferred to the Ar-purged ethanol solution of 4VP to undergo the UV irradiation. After the UV-induced coupling reaction, the silicon substrate was activated in PdCl₂ solution to selectively complex the Pd catalyst to the 4VP-patterned regions. The substrate was then immersed in an electroless copper plating bath to result in the deposition of copper metal in the selectively modified and activated regions. Figure 9a shows the optical microscopic image of the resist-patterned silicon surface. Figure 9b, on the other hand, shows the microscopic image of the selectively metallized silicon substrate with the square copper micropatterns, each having an area of $70 \times 70 \ \mu m^2$. Figure 10 shows the SEM images and EDX mapping of elemental Si (part a) and elemental Cu (part b) of the selectively metallized silicon substrate. The light areas show the distribution of the respective elements. The elemental maps of Figure 10 parts a and b complement each other every well, indicating a good resolution for the electrolessly deposited copper micropatterns on the surface-modified silicon substrate.

4. Conclusion

The H-terminated Si(100) substrate surface from HF etching could be further functionalized via the UV-induced coupling of a 4VP surface layer. Not only could the surface-coupled 4VP layer be used as chemisorption sites for the palladium complex during the Sn-free activation process for the electroless plating of copper but it also served as an adhesion promotion layer and diffusion barrier for the electrolessly deposited copper on the silicon surface. The Cu/4VP-modified Si assembly exhibited a 180×bc-peel adhesion strength of about 4 N/cm. The strong

Figure 10. SEM images and EDX mapping of (a) elemental Si and (b) elemental Cu of the micropatterned silicon substrate surface after selective modification and electroless plating of copper.

adhesion of the electrolessly deposited copper to the 4VP-modified silicon surface was attributed to the strong interaction of the pyridine functional groups of the 4VP layer with palladium and copper atoms and the fact that the 4VP layer was covalently tethered on the Si(100) surface. With the resist-patterned silicon substrates, the method could be used to produce adherent copper micropatterns directly on the silicon substrates.

References and Notes

(1) Rickerby, J.; Steinke, J. H. G. *Chem. Rev.* **2002**, *102*, 1525.
(2) Yung, E. K.; Romankiw, L. T.; Alkire, R. C. *J. Electrochem. Soc.* **1989**, *206*, 136.
(3) Li, J.; Shacham-Diamand, Y.; Mayer, J. W. *Mater. Sci. Reports* **1992**, *1*, 9.
(4) Nakahara, S.; Okinaka, Y. *Annu. Rev. Mater. Sci.* **1991**, *93*, 21.
(5) Dubin, V. M.; Shacham-Diamand, Y.; Zhao, B. *Mater. Res. Soc. Symp. Proc.* **1996**, *179*, 427.
(6) Shacham-Diamand, Y.; Dubin, V. M.; Angyal, M. *Thin Solid Films* **1995**, *93*, 262.
(7) Magagnin, L.; Maboudian, R.; Carraro, C. *Electrochem. Solid State Letter* **2001**, *4*, C5.
(8) Ye, S.; Ichihara, T.; Uosaki, K. *J. Electrochem. Soc.* **2001**, *148*, C421.
(9) Yeh, J. L. A.; Jiang, H. R.; Neves, H. P.; Tien, N. C. *J. Microelectromech. Syst.* **2000**, *9*, 281.
(10) Shacham-Diamand, Y.; Lopatin, S. *Electrochim. Acta* **1999**, *44*, 3639.
(11) Charbonnier, M.; Romand, M.; Kogelschatz, U.; Esrom, H.; Seebock, R. In *Metallized Plastics 7*: *Fundamental and Applied Aspects*; Mittal, K. L., Ed.; VSP: Utrecht, The Netherlands, 2001; p 3.
(12) Lin, J. H.; Tsai, Y. Y.; Chiu, S. Y.; Lee, T. L.; Tsai, C. M.; Chen, P. H.; Lin, C. C.; Feng, M. S.; Kou, C. S.; Shin, H. C. *Thin Solid Films* **2000**, *377*, 592.
(13) Kiang, M. H.; Lieberman, M. A.; Cheung, N. W. *Appl. Phys. Lett.* **1992**, *60*, 2767.

12516 *J. Phys. Chem. B, Vol. 106, No. 48, 2002*

Xu et al.

(14) Bhansali, S.; Sood, D. K.; Zmood, R. B. *Thin Solid Films* **1994**, *253*, 391.

(15) Hsu, H. H.; Lin, K. H.; Lin, S. J.; Yeh, J. W. *J. Electrochem. Soc.* **2001**, *148*, C47.

(16) Shacham-Diamand, Y. *Electrochem. Solid State Lett.* **2000**, *3*, 279.

(17) Kohn, A.; Eizenberg, M.; Shacham-Diamand, Y.; Sverdlov, Y. *Mater. Sci., Eng. A* **2001**, *302*, 18.

(18) Dressick, W. J.; Dulcey, C. S.; Geoger, J. H.; Calabrese, G. S.; Calvert, J. M. *J. Electrochem. Soc.* **1994**, *141*, 210.

(19) Dulcey, S.; Koloski, C. S.; Timothy, S. J.; Dressick, W.; Calvert, M.; Peek, J.; Brain, M. U.S. Patent 5,648,201, 1997.

(20) Zhang, Y.; Tan, K. L.; Liaw, B. Y.; Liaw, D. J.; Kang, E. T.; Neoh, K. G. *Langmuir* **2001**, *17*, 2265.

(21) Charbonnier, M.; Alami, M.; Romand, M. *J. Electrochem. Soc.* **1996**, *143*, 472.

(22) Charbonnier, M.; Romand, M.; Harry, E.; Alami, M. *J. Appl. Electrochem.* **2001**, *31*, 57.

(23) Chen, M. S.; Brandow, S. L.; Dulcey, C. S.; Dressick, W. J.; Taylor, G. N.; Bohland, J. F.; Georger, J. H.; Parelchek, E. K.; Calvert, J. M. *J. Electrochem. Soc.* **1999**, *146*, 1421.

(24) Bent, S. F. *J. Phys. Chem. B* **2002**, *106*, 2830.

(25) Zhang, W. C.; Strother, T.; Smith, L. M.; Hamers, R. J. *J. Phys. Chem. B* **2002**, *106*, 2656.

(26) Linford, M. R.; Fenter, P.; Eisenberger, P. M.; Chidsey, C. E. D *J. Am. Chem. Soc.* **1995**, *117*, 3145.

(27) Linford, M. R.; Chidsey, C. E. D *J. Am. Chem. Soc.* **1993**, *115*, 12631.

(28) Terry, J.; Linford, M. R.; Wigren, C.; Cao, R. Y.; Pianetta, P.; Chidsey, C. E. D. *Appl. Phys. Lett.* **1997**, *71*, 1056.

(29) Boukherroub, R.; Morin, S.; Bensebaa, F.; Wayner, D. D. M. *Langmuir* **1999**, *15*, 3831.

(30) Sieval, A. B.; Demirel, A. L.; Nissink, J. W. M.; Linford, M. R.; van der Maas, J. H.; de Jeu, W. H.; Zuilhof, H.; Sudholter, E. J. R. *Langmuir* **1998**, *14*, 1759.

(31) Lee, E. J.; Bitner, T. W.; Ha, J. S.; Shane, M. J.; Sailor, M. J. *J. Am Chem. Soc.* **1996**, *118*, 5375.

(32) van der Putten, A. M. T.; de Bakker, J. W. G.; *J. Electrochem. Soc.* **1993**, *140*, 2229.

(33) Dressick, W. J.; Dulcey, C. S.; Georger, J. H.; Calvert, J. M. *Chem. Mater.* **1993**, *5*, 148.

(34) Vargo, T. G.; Gardela, J. A.; Calvert, J. M.; Chen, M. S. *Science* **1993**, *262*, 1711.

(35) Hampden-Smith, M. J.; Kodas, T. T.; *Chem. Vap. Deposition* **1995**, *1*, 8.

(36) Jeon, N. L.; Nuzzo, R. G.; Xia, Y.; Mrksich, M.; Whitesides, G. M. *Langmuir* **1995**, *11*, 3024.

(37) Wade, C. P.; Chidsey, C. E. D. *Appl. Phys. Lett.* **1997**, *71*, 1679.

(38) Zhang, J. F.; Cui, C. Q.; Lim, T. B.; Kang, E. T.; Neoh, K. G. *Chem. Mater.* **1999**, *11*, 1061.

(39) Ebneth, H. Metallizing of plastic. In *Handbook of Theory and Practice*; Suchentrunk, R., Ed.; ASM International: Materials Park, OH, 1993; p 30.

(40) Lee, E. J.; Ha, J. S.; Sailor, M. J. *J. Am. Chem. Soc.* **1995**, *117*, 8295.

(41) Green, W. H.; Lee, E. J.; Lauerhaas, J. M.; Bittner, T. W.; Sailor, M. J. *J. Appl. Phys. Lett.* **1995**, *67*, 1468.

(42) Cleland, G.; Horrocks, B. R.; Houlton, A. *J. Chem. Soc., Faraday Trans.* **1995**, *91*, 4001.

(43) Kim, N. Y.; Laibnis, P. E. *J. Am. Chem. Soc.* **1997**, *119*, 2297.

(44) Lee, E. J.; Bitner, T. W.; Hall, A. P.; Sailor, M. J. *J. Vac. Sci. Technol. B* **1996**, *14*, 2850.

(45) Moulder, J. F.; Stickle, W. F.; Sobol, P. E.; Bomben, K. D. In *X-ray Photoelectron Spectroscopy*; Chastian, J., Ed.; Perkin-Elmer: Eden Prairie, MN, 1992; p 43.

(46) Cicero, R. L.; Linford, M. R.; Chidsey, C. E. D. *Langmuir* **2000**, *16*, 5688.

(47) Holmes-Farley, S. R.; Whitesides, G. M. *Langmuir* **1987**, *3*, 120.

(48) Tan, K. L.; Woon, L. L.; Wong, H. K.; Kang, E. T.; Neoh, K. G. *Macromolecules* **1993**, *26*, 2832.

(49) Yang, G. H.; Kang, E. T.; Neoh, K. G.; Zhang, Y.; Tan, K. L. *Langmuir* **2000**, *117*, 211.

(50) Lyons, A. M.; Vasile, M. J.; Pearce, E. M.; Wasaeza, J. V. *Macromolecules* **1988**, *21*, 305.

(51) Jackson, R. L. *J. Electrochem. Soc.* **1990**, *137*, 95.